Structural and Multidisciplinary Optimization (2023) 66:189
https://doi.org/10.1007/s00158-023-03644-3

RESEARCH PAPER

Multi-objective parametric optimization of a composite high-performance prostheses using metaheuristic algorithms

Hyan Cândido Guedes[1] · João Luiz Junho Pereira[2] · Guilherme Ferreira Gomes[1]

Received: 19 April 2023 / Revised: 5 July 2023 / Accepted: 21 July 2023 / Published online: 9 August 2023

Abstract

With the rapid advancement of technology and computing, numerous processes and products have been developed to achieve improved performance at a lower cost and/or reduced material usage. Orthopedic prostheses, benefiting from the discovery of new materials, have witnessed continuous evolution and optimization. Therefore, this study aims to develop and parametrically optimize a high-performance composite material using the interpolation strategy of splines and keypoints, thickness variations, and the number of layers, resulting in 16 decision variables. Furthermore, the performance of four different multi-objective optimizers was evaluated in the optimization process: NSGA-II, MOLA, MOSFO, and MOPSO. The study aimed to minimize the total mass and evaluate the Tsai–Wu failure criterion under two different loading conditions. The numerical results obtained through the finite element method and optimization led to different convex Pareto fronts. The MOPSO algorithm demonstrated superior robustness compared to the other metaheuristic algorithms evaluated. As a result, the optimal solution obtained using MOPSO was substantially improved compared to the initial model, indicating the effectiveness of this approach in optimizing the high-performance composite material for the specific problem under consideration.

Keywords Multi-objective optimization · Prosthesis · Composites · Finite element

List of symbols

MOGA	Multi-objective Genetic Algorithm
MOLA	Multi-objective Lichtenberg Algorithm
MOSFO	Multi-objective SunFlower Optimization Algorithm
MOPSO	Multi-objective Particle Swarm Optimization Algorithm
PSO	Particle Swarm Optimization
TW	Tsai–Wu failure index
HV	Hypervolume
X_k	Newton's method objective function variable
X_{k+1}	Future value of
$f_i(X)$	Objective function to be minimized
$g_k(x)$	Problem restriction
$h_j(X)$	Problem restriction
x_i	Decision variables
M	Number of problem objectives
N	A generic population
R_d	Real space of dimension d
N_s	Undominated solutions
p_p	Pollination rate
M	Mortality Rate
s	Sunflower Survival Rate
x_n	Decision variable in x from point n
y_n	Decision variable in y from point n

1 Introduction

Engineering has always sought to optimize and improve processes and their constructions. The relief of weight associated with the good performance of a machine or tool is one of the many challenges within engineering, because it means lower spending on material and better use of it. Furthermore, lighter structures become easier to handle and bring several other benefits depending on their applications. For example, regarding motoring, weight relief means better performance in curves and better acceleration, because the engine will have to work less to break the inertia of the vehicle and

Responsible Editor: Gang Li.

✉ Guilherme Ferreira Gomes
guilhermefergom@unifei.edu.br

[1] Mechanical Engineering Institute, Federal University of Itajubá, Itajubá, Brazil

[2] Computer Science Division, Aeronautics Institute of Technology (ITA), São José Dos Campos, Brazil

to leave the static state. However, it is not only within the field of high-performance engineering that mass reduction is beneficial. In medicine, the use of lightweight prostheses brings several benefits to its users (Ma et al. 2020), because it enables better locomotion (Carbonaro et al. 2021). For example, according to Lourenço (2019) a lower limb prosthesis should be lightweight to minimize energy expenditure and muscle effort, considering the biomechanical changes in gait that cause greater energy expenditure.

Choosing the appropriate material is a key factor in reducing the mass and improving the performance of a prosthesis. Historically, prostheses have been made from a variety of materials, including animal bones and wood. With the discovery of metals, ferrous alloys became a popular choice, and in ancient Greece they were often produced by the same blacksmith who crafted armor.

With the rapid advancement of technology and computing, numerous processes and products have been developed to achieve improved performance at a lower cost and/or reduced material usage. Orthopedic prostheses, benefiting from the discovery of new materials, have witnessed continuous evolution and optimization. Multi-objective optimization has played a crucial role in the development of these prostheses, allowing the search for efficient and balanced solutions across multiple performance criteria (Diniz et al. 2019; Francisco et al. 2021; Pereira et al. 2022ab).

Multi-objective optimization involves the simultaneous search for multiple conflicting objectives, taking into account the trade-offs between them. Unlike single-objective optimization, where a single solution is sought, multi-objective optimization aims to find a set of optimal solutions, known as the Pareto front, which represents the trade-off among the considered objectives.

In recent years, various multi-objective optimization approaches have been proposed in the scientific literature. Metaheuristic-based algorithms have proven particularly suitable for solving complex multi-objective optimization problems due to their ability to efficiently explore the search space and find high-quality solutions. Some examples of widely used metaheuristic algorithms include NSGA-II (Non-dominated Sorting Genetic Algorithm II), MOLA (Multi-Objective Lichtenberg Algorithm), MOSFO (Multi-Objective Sunflower Optimization Algorithm), and MOPSO (Multi-Objective Particle Swarm Optimization).

For example, a multi-criteria optimization model was developed by Ruben et al. (2007) in order to obtain the optimal geometry of the femoral component of a hip prosthesis. The objective function minimizes both the relative tangential displacement and the contact normal stress. The three-dimensional optimization procedure developed allows us to characterize the stem shape that minimizes displacement and stress individually or simultaneously using a multi-criteria approach. Results show that thin stem tips minimize the interface stress while collared stems minimize displacement. The author concluded that the multi-criteria formulation leads to balanced solutions.

Rosel Solis et al. (2021) used a crow search algorithm (CSA) to optimize a running blade made of composite materials. The optimization objective was to increase RBP displacement while considering the Tsai–Wu failure criterion. Displacement and the Tsai–Wu criterion were predicted using artificial neural networks (ANN) trained with FEM simulations. The authors concluded that the carbon fiber layers with layers oriented 0°/90° were the best option for the design of the RBP and the proposed methodology can reduce the manufacturing costs of the final structure.

Equally important, Chanda et al. (2016) presented a multi-criteria 3D shape optimization for both long-term and post-operative failure criteria associated with cementless hip prostheses design. From the final obtained Pareto optimal solutions, two chosen trade-off models were analyzed later. Despite the limitations, the multi-objective optimization results obtained by the authors attempt to address three key failure mechanisms to understand the design rationale of cementless hip prostheses.

Running-specific prosthetic feet, designed to enhance performance by storing and releasing elastic energy, have gained significant attention in the field of prosthetics. Shepherd et al. (2022) performed finite element analyses in order to demonstrate the influence of prosthesis shape on its multidimensional and non-linear mechanics. The authors proposed a novel approach that combines simple formulations for foot mechanics with a spline-based shape optimization technique. By optimizing the shape based on desired endpoint mechanics, the methodology was able to generate new prosthetic foot designs that can improve performance and biomechanics for individuals with lower limb amputations.

Currently, prostheses are made of materials that combine lightness and mechanical strength, as shown by Light (2000) in his article "Development of a lightweight and adaptable multiple-axis hand prosthesis." In the present study, the prosthesis material will be carbon fiber, which is widely used in applications that require the mentioned characteristics, such as in the aeronautic and automotive industries, and in other applications that seek self-performance, as already mentioned, in motor racing.

Different final tasks and conditions require prosthetic foot devices with varying stiffness. According to this, Tryggvason et al. (2020) presented a case study focused on modifying the design of a prosthetic foot to achieve variable stiffness. The objective was to demonstrate the proof-of-concept by using finite element modeling to simulate the design modifications where the goal was to adjust the stiffness of the device under dynamic loading by applying a high damping constant that approaches force coupling for the specified boundary conditions. The results demonstrated that the

introduction of a high damping constant damping element can increase the overall rotational stiffness of the device by 50%. Furthermore, with a sufficiently large damping coefficient, the energy dissipation in the active element accounts for approximately 20% of the maximum strain energy.

Furthermore, the choice of material is not the only factor that implies the reduction of mass and the improvement of the performance of a prosthesis. Within solid mechanics, the dimensions imply directly in the resistance to stresses. A poorly dimensioned geometry means that a design must have greater mass to resist the same forces than a well dimensioned geometry.

In the field of lower limb prostheses, this study is still scarce and there is still much to be developed. As mentioned before, combining mass and mechanical strength is not an easy task and must be studied carefully. There are various methods to optimize these two parameters, including topological optimization based on the material's points of maximum stress, as demonstrated in Zhen Tao's study (2017). However, topological optimization is still a challenge for the development of carbon fiber prostheses and structures due to the orthotropic characteristic of the materials. In this case, parametric optimization is more suitable. Nevertheless, the research and the development of prostheses with this type of optimization are even scarcer.

Given this problem, it is perceptible that there is a lack of studies in this area. Thus, the present work seeks to develop a study on the multi-objective optimization of a high-performance foot prosthesis made of composite material. In terms of structural design, multi-objective optimization has been applied to optimize the shape and dimensions of a prosthetic foot. This study aims to improve the structural integrity, reduce weight, and enhance the biomechanical compatibility of the prosthetic devices. When considering various objectives such as Tsai–Wu failure criterion and weight reduction, innovative designs result in better performance and greater user comfort.

The main objective of this study is to develop a carbon fiber foot prosthesis and optimize it using a parametric approach. To achieve this, the following steps were undertaken: (1) Development of a parametrized finite element model that accurately represents the prosthesis geometry and properties; (2) Application of appropriate boundary conditions that simulate realistic loading conditions on the prosthesis; (3) Integration of the model with four multi-objective optimization algorithms, namely Multi-objective Lichtenberg Algorithm (MOLA), Multi-objective Genetic Algorithm (MOGA), Multi-objective Particle Swarm Optimization (MOPSO), and Multi-objective Sunflower Optimization (MOSFO); and (4) Determination of the optimal design that minimizes both the mass and the Tsai–Wu failure index, which are critical factors in ensuring that the prosthesis meets performance requirements.

2 Theoretical background

2.1 High-performance composite prosthesis

As the name already says, they are prostheses that seek maximum performance. That is, less mass and more efficiency, besides a profile that resists well to the impacts during a walk or run, avoiding major problems to the user (Venkadesan et al. 2020).

Contrary to popular belief, performance prosthetics are not exclusively designed for athletes, as is often the case with orthopedic prosthetics for runners. They are also suitable for individuals who seek greater comfort while walking or running. This is because, as demonstrated by Oudenhoven's research (2017), performance prosthetics must exhibit similar properties to that of a human leg, particularly with regard to stiffness.

Figure 1 shows a comparison between the anatomy of a human foot, highlighting the arches, and an arbitrary profile of the prosthesis modeled numerically in this study. From the two images it is possible to note the similarity between the two profiles, as the focus of the study was to develop and optimize a prosthesis that follows the pattern of a real foot.

2.2 Composite structures

By definition, composites are the union of two or more distinct materials with the objective of forming a third material that has specific characteristics of the materials used, such as high hardness and low density. In addition, composites are made up of two basic phases:

- Matrix: which can be ceramic, metallic, or polymeric. Generally, metals and polymers are chosen as the matrix materials, for presenting ductility, a characteristic that is frequently required by the industry.
- Reinforcement: may be particles or fibrous material.

From this phase of matrix and reinforcement, one can work with the proportions and/or characteristics of each to achieve the required properties, such as higher mechanical resistance, resistance to temperature, higher hardness, flexibility, among others.

In the regions that separate these phases (the so-called interfaces), we have different properties from the other two phases, thus opening up a very wide range of possibilities. In addition, what sets composites apart from other materials that can also be combined (metal alloys, for example) is the fact that the combination is done macroscopically, that is, seen with the naked eye.

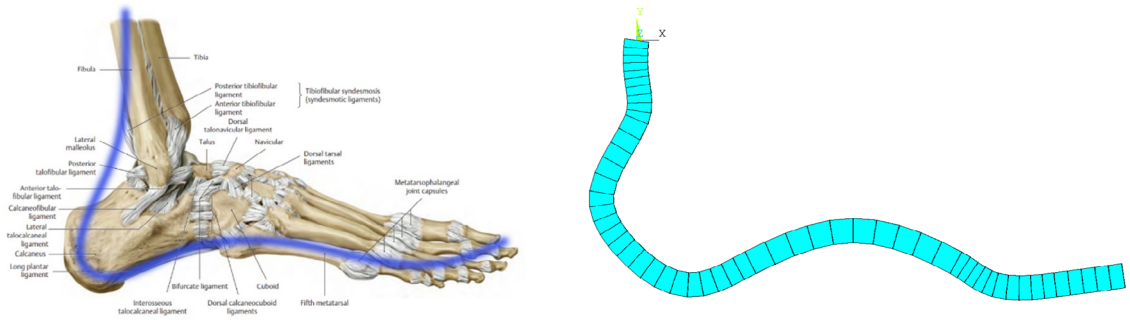

(a) Anatomy of a human foot (adapted from Ricciardi, 2015)

(b) an arbitrary profile of the modeled structure

Fig. 1 Comparison between the **a** profile of a human foot and the **b** prosthesis developed in this work

Nowadays, composite materials are widely used in different types of industries, among them: aeronautic, automotive, and construction.

However, the applications of composite materials are not limited to these three areas. Due to the combination of low density and high mechanical strength of some of these materials, as is the case of carbon fiber, many orthopedic prostheses are developed and manufactured in composite material.

2.3 Optimization

According to Yang (2014), optimization is widely used and quite essential in several activities, such as business, industrial production, and, undoubtedly, engineering projects. The first optimization methods were based on deriving a function to be optimized, and thus obtaining the maximum or minimum value of that function. However, this method has errors, since within a function there are several local maximum and minimum points and only one global minimum and one global maximum.

A classic and rather old example based on derivatives is Newton's method (Eq. 1), which can be used for functions of one variable, where X_{k+1} is a future value that will be obtained from a present value X_k, where the first value will be a guess X_1, $f(X_k)$ is the objective function to be minimized in X_k , and $f\prime(X_k)$ its first-order derivative:

$$X_{k+1} = X_k - \frac{f(X_k)}{f(X_{k+1})}. \tag{1}$$

The iterative process above takes the function to a minimum value near the initial guess which can be a local or global minimum. Deriving this procedure we have the Newton–Raphson method.

The problem with these classical methods, as can be seen, is that it is limited to functions that are continuous and derivable near the local minimum. Thus, these methods do not fit most real problems.

Mathematically speaking, according to Yang (2014), it is possible to write most optimization problems in generic form:

$$minimize\, f_i(x), \quad (i = 1, 2, 3, \ldots, M),\ x \in R^d \tag{2}$$

$$subject\ to\ h_j(x) = 0, \quad (j = 1, 2, 3, \ldots, J) \tag{3}$$

$$g_k(x) \leq 0, \quad (k = 1, 2, 3, \ldots, K), \tag{4}$$

where $f_i(x)$, $h_j(x)$, and $g_k(x)$ are functions of the vector

$$x = \left(x_1, x_2, x_3, \ldots, x_d\right)^T. \tag{5}$$

Here, the components x_i of x are called decision variables, and they can be real continuous, discrete, or a mixture of these two.

Also according to Yang (2014), the functions $f_i(x)$, where $i = 1, 2, 3, \ldots, M$ are called objective functions, and in the case of $M = 1$, there is a single objective. The space generated by the decision variables is called the design space or search space R^d, whereas the space formed by the objective function values is called the solution space or response space. The equalities for h_j and the inequalities for g_k are called constraints. It is worth noting that we can also write the inequalities in another form, ≥ 0, and we can also formulate the objectives as a maximization problem.

2.3.1 Multi-objective optimization

Multi-objective optimization, also known as multi-criteria optimization or Pareto optimization, is the process of optimizing multiple objectives or criteria simultaneously. This approach is used when there is no single-objective function

that can adequately represent all the goals of the optimization problem.

In multi-objective optimization, the goal is to find a set of solutions that are Pareto optimal. A Pareto optimal solution is one where any improvement in one objective function would result in a deterioration in at least one other objective function. In other words, a Pareto optimal solution cannot be improved in one objective without worsening at least one other objective. Multi-objective optimization problems are commonly encountered in engineering and design problems, where the design goals often involve multiple criteria that need to be satisfied simultaneously.

There are several methods and algorithms that can be used to solve multi-objective optimization problems. These include traditional methods such as weighted sum, epsilon constraint, and goal programming, as well as more modern approaches such as evolutionary algorithms, swarm intelligence, and machine learning. Evolutionary algorithms are popular for solving multi-objective optimization problems because they can effectively explore the search space and find a set of Pareto optimal solutions. Common evolutionary algorithms used for multi-objective optimization include genetic algorithms, particle swarm optimization, and differential evolution.

Basically, multi-objective optimization of a process is to optimally and/or evenly combine two or more variables chosen to be improved, usually in conflict with each other. An easy and intuitive example to understand what optimization is the purchase of a cell phone. The price and the quality of the handset are conflicting characteristics, because usually a handset with a lot of features and excellent performance normally has a higher price when compared to a lower quality handset. The optimal choice will depend on the consumer, and they may choose the most expensive one with the best performance, one with lower performance and lower price, or a balance point between the two features, that is, the best value for money. However, among all the equipment configurations there are some that are superior to others, that is, they present higher or equivalent performance for a lower or equal cost. These configurations (solutions) that surpass others are known as non-dominated solutions, while the configurations that are surpassed by at least another one are known as dominated solutions (Kaveh and laknejadi 2011, 2013).

2.3.2 Multi-objective lichtenberg algorithm (MOLA)

One metaheuristic based on the lightning storm and Lichtenberg figures was recently created in the mono-objective version and expanded to its multi-objective version, which is what interests us in the present study. Pereira et al. (2021a, b) and Pereira et al. (2022a, b) present and detail the whole study behind the mono- and multi-objective optimizer, respectively.

In short, the algorithm consists of creating a Lichtenberg figure that is thrown into the search space, and points of its structure are taken as candidates for the evaluation of the objective functions.

According to Pereira et al. (2022a, b), Lichtenberg (1777) was the first to study this phenomenon of propagation of electrical discharges in dielectric material (resistant) that leads the figure to have branched and tortuous aspects. This happens because the material is not homogeneous and, therefore, the growth of these rays appears randomly even under the same electrostatic conditions. This growth has an indescribable physical and mathematical reason. And, until today, it is impossible to calculate and predict it.

The direction of the lightning depends on the temperature, density, pressure and humidity of the air, the dielectric environment, the type of soil below the cloud, the density of that cloud, the velocity of the particles within it and what types they are, whether or not there are oxides, finally, a wide variety of variables with a single result: a stochastic event that spreads in the direction of least resistance. Lichtenberg Figure can be constructed through a random growth process with many particles, forming a cluster. Due to its stochastic model, each run of the algorithm can generate different figures. Therefore, the construction of the Lichtenberg Figure is entirely numerical.

2.3.3 Non-dominated sorting genetic algorithm (NSGA-II)

This algorithm was first proposed by Fonseca and Fleming in 1993, and is a multi-objective optimization method based on genetic algorithms for generating the set of non-dominated solutions.

This algorithm works as follows: a population Z of size N is generated. Using selection, recombination, and mutation, a population of offspring of the same size as Z is generated. After that, the two groups are put together and we have a set of size $2N$. Then, they are sorted into dominance fronts and the clustering distances on each front are evaluated. Then the final descendants are determined by selecting the fronts with the best degree of dominance. If the size limit N is exceeded, the solutions with the smallest clustering distance on the last selected front are eliminated. Thus, if the convergence criterion is reached, end of process. Otherwise, one set is again joined to another forming a new one of size $2N$.

2.3.4 Multi-objective particle swarm optimization (MOPSO)

From the observation and study of the social behavior of schools of fish, migratory bird species, and humans, the

Particle Swarm Optimization (PSO) algorithm was developed by James Kennedy and Russell Elberhart in 1995.

According to Kennedy and Eberhart, two concepts govern the performance of the algorithm: one is the ability of each particle (individual of a population) to quantify the effectiveness of its own experience, called cognitive learning, and the iterative exchange of experiences with its neighbors, labeled as social learning. As such, a particle traverses the solution space with velocity of displacement consequent to social–cognitive learning.

In this algorithm, the particles walk in a space R_d, where d is the dimension of the space. The changes in the attributes of that particle lead to new positions in that space. These changes occur as a consequence of the already-mentioned social–cognitive behavior.

2.3.5 Multi-objective sunflower optimization (MOSFO)

The multi-objective sunflower algorithm (or SunFlower Optimization Algorithm) is similar to its mono-objective version (Gomes et al. 2019; Gomes and Almeida 2020). Initially, the algorithm generates a first population of n sunflowers (population), which are randomly ordered in the size of the search space. Then, MOSFO (Multi-objective SunFlower Optimization) computes the fitness of each sunflower using each of the objective functions of the problem. Each decision vector in the search space generates a solution in the objective space, which is divided into hypercubic grids (Coello et al. 2000). The Pareto dominance relation is performed and these solutions are divided into dominated and non-dominated solutions. The dominated solutions are excluded and Ns non-dominated solutions form the first Pareto front of the algorithm, which becomes the sunflowers sun and is saved.

Since sunflowers in nature are guided by the sun during the day, in this optimization technique sunflowers are oriented by the current Pareto front. Once all individuals are oriented by the sun, the individuals in a random and orderly way will generate new individuals towards it. This occurs via three MOSFO parameters, called biological operators: (i) pollination rate (p_p), (ii) mortality rate (m), and (iii) sunflower survival rate (s). At each iteration or day (of the number of iterations N days), the pollination rate determines the proportion of individuals in a population that cross-pollinate with each other. It is worth noting that the best individuals cross-pollinate hierarchically, chosen at random at the minimum distance between flower i and flower $i+1$. For simplicity, each sunflower produces only one pollen gamete and reproduces individually.

The plant mortality rate determines that a percentage of the individual will not survive because they are away from the sun and, therefore, have not received enough energy to be sustained. Individuals m (%) will be selected as the worst individual in their population based on their fitness value. Thus, the percentage of surviving plants will move in a controlled manner towards the sun. Even though in nature sunflowers do not move, in this algorithm, a movement is assigned to each individual. The range of movement will be random, following a normal distribution, between its position and the position of the sun. Figure 2 compiles the summarized flowchart of all the multi-objective algorithms discussed in this study.

3 Methodology

The constructive model of the prosthesis previously defined was that the structural part of the prosthesis, in other words, the object of study of this work, would consist of three identical carbon fiber strips that would be placed inside a

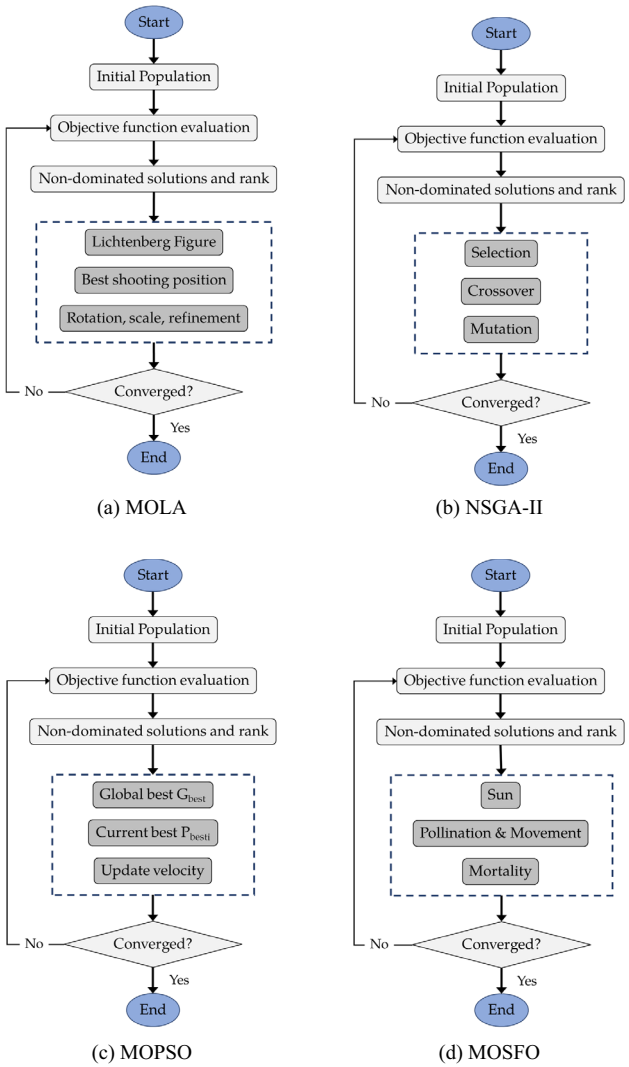

Fig. 2 Summary flowcharts of the multi-objective algorithms NSGA-II, MOLA, MOPSO, and MOSFO

3D printed foot. For these reasons, the dimensions of these strips should respect the dimensions of the printed foot (or customized according to the size of the foot of the individual receiving the prosthesis). In addition, the prosthesis will be subjected to loading conditions (i) at the foot and (ii) at the heel, and, subsequently, analyzed numerically to obtain the stresses and Tsai–Wu failure index.

3.1 Direct problem: finite element formulation

At first the case study was isolated for only one strip and all the information obtained for this one will be taken as results for the other two strips as well. Moreover, in order to simplify the analysis, the whole prosthesis was built in shell elements.

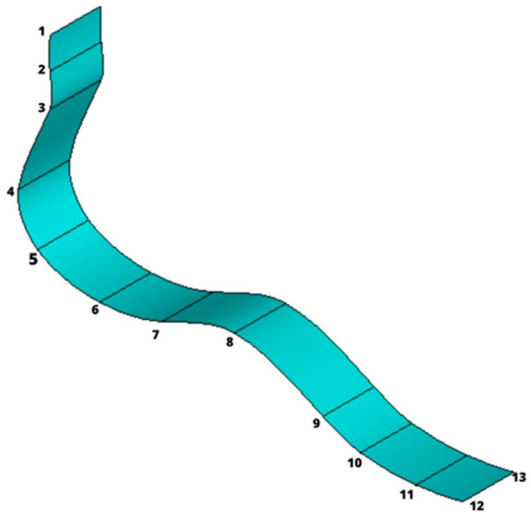

Fig. 3 An arbitrary profile obtained for the prosthesis

After the initial considerations and the boundary conditions already explained, in Ansys® APDL a profile of a strip of the prosthesis was created from random points that would generate a profile visually similar to that of a prosthesis and that respected the geometric limits imposed. For this, 13 points (keypoints) were defined with coordinates in the x–y plane. Figure 3 shows the 12 points responsible for generating the structural profile of the prosthesis (points 1 to 12). The points were connected by means of a spline and an area was generated considering a Z thickness (points 12 to 13).

Regarding the numerical model, we sought to build a simple structured mesh and sufficient elements in order to obtain reliable results and with the shortest possible simulation processing time, since, a posteriori, several prostheses will be simulated (objective function evaluation) until reaching the optimal model. Thus, we arrived at a mesh of 275 elements with 8 nodes per element.

Once the mesh was built, the boundary conditions were defined, which were done in two different cases. One with the strength applied to the tip of the prosthesis, and a second case with the strength applied to the heel. The first with a value of 400 kgf and the second of 500 kgf, given by standard, were divided equally in the three carbon fiber strips. It is worth noting that these forces were distributed at the nodes located in the regions of interest (Perl et al. 2012). Beyond this applied force, the ankle region of the prosthesis was crimped in both the cases. Figure 4 shows the two boundary conditions evaluated in this study.

3.2 Optimization problem: modeling and formulation

As already mentioned in the previous paragraphs, the main objective of this study is to optimize a carbon-epoxy prosthesis that is as light as possible and structurally safe.

However, before starting the optimization, it is necessary to simplify it as much as possible and in the best possible way, so that there is no waste of time and uninteresting results for our study. Thus, it is known that the optimization of the profile must happen respecting the 13 keypoints that have freedom in the three dimensions (X, Y, and Z axes). From this point on 39 decision variables would be present for the objective functions that are to minimize mass and Tsai–Wu. This number of variables would not be ideal for an optimization problem. So, the need to simplify the problem is confirmed.

Knowing the boundary conditions and geometric limits that the prosthesis must respect, some variables were fixed and dependency was created between them. In this way, the number of decision variables was reduced from 40 (39 geometric freedoms plus the number of fiber layers) to 16.

Thus, following what is shown in Eqs. 3, 4, the optimization problem statement of this study can be summarized by Eqs. 4.

$$find\{X\} = \{y_3, x_4, y_4, x_5, y_5, x_7, y_7, x_8, y_8, x_9, y_9, x_{10}, x_{11}, y_{12}, z_{13}, N_{CAM}\} \quad (6)$$

$$that\ minimizes : f_1(X) = TW(X) \rightarrow Tsai - Wu'svalue \quad (7)$$

$$f_2(X) = mass\,(X) \rightarrow Mass\ value \quad (8)$$

$$subject\ to : g_1(X) : mass\,(X) \leq 550 \quad (9)$$

$$g_2(X) : TW(X) \leq 1 \quad (10)$$

$$where : LB \leq \{X\} \leq UB \quad (11)$$

Visually, the design vector X composed of the decision variables considered in this study can be seen in Fig. 5. At the same time, the considerations about the decision

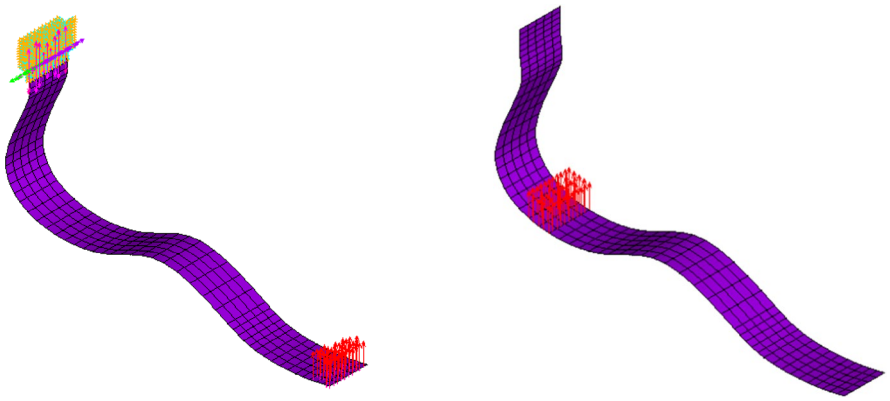

(a) simulated prosthesis with strength on the tip (b) simulated prosthesis with strength on the heel

Fig. 4 Load application points on the prosthesis

variables, $\{X\}$, and their limits (lower and upper) can be seen in Table 1 and Table 2.

It is also worth mentioning that besides the points for the formation of the lateral structural profile, the prosthesis thickness (z_{13}) was considered in the formulation of the optimization problem as well as the number of layers along the thickness (N_{CAM}). All layers are oriented at 0° along the longitudinal direction of the prosthesis. Furthermore, for all optimization cases, the N_{CAM} variable was considered as the integer variable to be optimized.

It is worth noting that in Table 1 many values are negative because the reference axis in the construction of the prosthesis was fixed in the ankle region. That is, all points in y are below the axis, therefore, negative.

Furthermore, in the four optimizers used, it is necessary to define upper and lower bounds for the values of each decision variable. These values can be seen in Table 2 and were defined considering the shape to which the prosthesis is limited, and we tried to keep it as close as possible to the previously built shape.

Regarding the optimizers considered, Table 3 shows the main internal control factors used. As a comparative study, for all cases it was defined as a stopping criterion the maximum amount of objective function evaluation or simply the iterations, since the population of individuals is the same for all.

In addition, these algorithm-specific MO algorithms were chosen due to some reasons. First, these algorithms have been shown to be effective in other studies involving composite

Table 1 Keypoints and formulation of the geometric construction of the prosthesis

	X (m)	Y (m)	Z (m)
Point 1	0	0	0
Point 2	0	− 0.02045	0
Point 3	0	y_3	0
Point 4	x_4	y_4	0
Point 5	x_5	y_5	0
Point 6	$(x_7+x_5)/2$	− 0.13497	0
Point 7	x_7	y_7	0
Point 8	x_8	y_8	0
Point 9	x_9	y_9	0
Point 10	x_{10}	− 0.13497	0
Point 11	x_{11}	− 0.13497	0
Point 12	0.26994	y_{12}	0
Point 13	0.26994	y_{12}	z_{13}

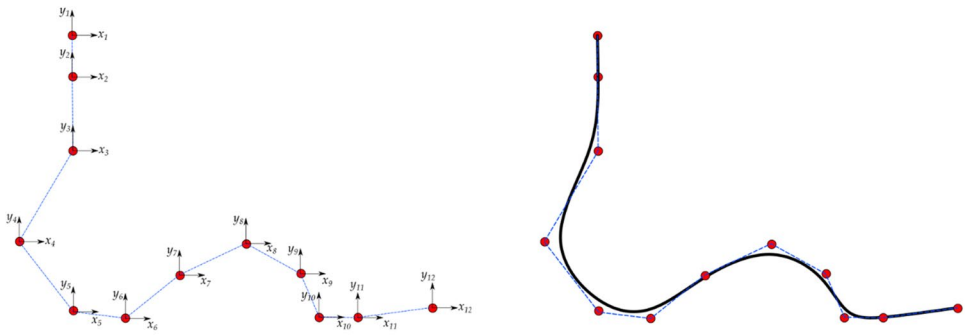

(a) (b)

Fig. 5 Details about modeling and parameterization of the direct model

Table 2 Limits of the decision variables

Variable	Upper bound (UB)	Lower bound (LB)
y_3 (m)	− 0.0320	− 0.0552
x_4 (m)	0.0020	− 0.0409
y_4 (m)	− 0.0700	− 0.0981
x_5 (m)	0.0000	− 0.0123
y_5 (m)	− 0.0981	− 0.1309
x_7 (m)	0.0800	0.0460
y_7 (m)	− 0.1145	− 0.1309
x_8 (m)	0.1300	0.1100
y_8 (m)	− 0.1000	− 0.1100
x_9 (m)	0.1841	0.1700
y_9 (m)	− 0.1145	− 0.1309
x_{10} (m)	0.2126	0.1850
x_{11} (m)	0.2515	0.2127
y_{12} (m)	− 0.1288	− 0.1309
z_{13} (m)	0.0500	0.0200
N_{CAM}	100	50

Table 3 Control factors of the optimizers

	MOLA	NSGA-II	MOPSO	MOSFO
Population	160	160	160	160
Refinement Ref	0,40	–	–	–
Particles N_p	10^6	–	–	–
Stick S_c	1	–	–	–
Radius R_c	150	–	–	–
Crossover	–	60%	–	–
Mutation	–	5%	–	–
Inertia W	–	–	0,4	–
Cognitive C_1	–	–	2	–
Social C_2	–	–	2	–
Pollination p	–	–	–	10%
Mortality m	–	–	–	10%
Iterations	100	100	100	100

materials and/or orthopedic prostheses. This suggests that they are well suited to the specific problem being addressed in the study. Secondly, the authors may have chosen to use these four algorithms because they represent a diverse set of metaheuristic algorithms, each with its own strengths and weaknesses. By evaluating multiple algorithms, the authors can compare their results and determine which algorithm is the most effective for their specific problem.

4 Numerical results and discussion

Based on the information and data presented in the previous sections, numerical simulations and optimizations were carried out using the four metaheuristic optimizers mentioned earlier for two different boundary conditions applied to the prosthesis. That is, there were 8 simulations that generated a total of 779 different optimal configurations (non-dominated solutions on the Pareto front). Then, using specific decision-making techniques, 8 optimal prostheses were obtained, improving both TW and mass. Besides these 8 prostheses, another 16 prostheses were obtained: 8 of them targeting only TW and 8 targeting only the mass of the prosthesis. The latter 16 refers to the nadir points obtained by each optimizer.

Furthermore, for a first study before the simulation in the optimizers, having the upper and lower bounds of each decision variable, some examples of combination with these bounds were randomly generated, which can be seen in Fig. 6. As can be seen, different combinations of the decision variables can result in different structural designs, which directly impact the evaluated mass and Tsai–Wu responses. In addition to this example, the variables thickness (z_{13}) and number of layers (N_{CAM}) contribute significantly to these responses.

4.1 Analysis of variance and sensitivity

One of the ways to verify and analyze the influence of a given variable on a particular problem is through the analysis of variance and sensitivity. Through it, it i s possible to know how the objective functions, mass and TW, of the problem behave in relation to the decision variables previously shown and how they are distributed, as well as in a histogram.

Moreover, for the initial sensitivity and variance analyses, a design of experiments was performed using a 2^{16} factorial arrangement resulting in 65,536 different combinations of variables. These 65,536 different configurations were then simulated and the mass and TW responses for each case were stored.

By the violin plot shown in Fig. 7 it is possible to see that the average mass of the prostheses obtained was something close to 300 g, while the mass response with the highest density in the sample space was something slightly greater than 100 g.

Still in the violin plot, now analyzing the TW, it is possible to see that the average TW was between 2 and 4, which is not interesting, because this value should be below one to ensure that the prosthesis does not reach failure. Note that this average is due to the fact that there are outliers—data that are very distant from the other data—of very high TW, which affects the calculation of the average TW, since these outliers reached a value of 20 for TW, while the ideal is below 1, as mentioned. However, there is a higher density of results at TW between 0 and 3, especially close to 2. That is, arriving at an optimal value that

Fig. 6 Some examples of prostheses generated for different structural parameter settings

leads to a TW smaller than one is not an easy task, since few answers meet this requirement.

Besides the violin plot, a sensitivity analysis can be done through Fig. 8 and Fig. 9, which show how the mass and TW behave varying only one variable between their lower and upper limits.

For the mass it is possible to see that the parameters with the greatest influence are the last two, which are the width of the "strip" and the number of layers that directly influence the thickness and thus add weight to the prosthesis. In other words, the shape of the lateral profile of the prosthesis was of little importance, because by varying the parameters from y_3 to y_{12} there was very little variation in mass. Some

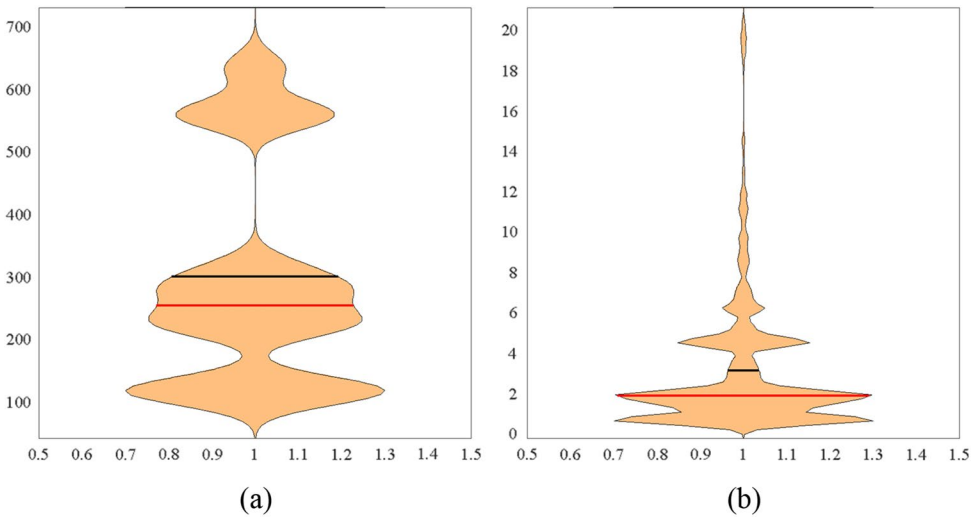

Fig. 7 Violin plot for the responses of mass (**a**) and Tsai–Wu (**b**)

parameters, such as y_3 and y_4, did not even vary the value of the mass by changing them. This happened because moving the points that generate the profile of the prosthesis does little to change its final length, that is, it will add almost no mass to it.

Nevertheless, for TW (Fig. 9), not only the last decision variables were important, but also most of the decision variables. However, similarly, here too the parameters with the greatest influence were the width of the prosthesis and the number of beds. Nevertheless, this time the relationship is the other way around, meaning that if we increase the number of layers and/or the width, we will get a lower TW for the simulated prosthesis. Although, the mass will increase as well.

In addition, the decision variables x_4, y_4, x_9, x_{11}, and x_{12} were, among the variables that design the profile of the prosthesis, the parameters that most influenced the control of tension in the material studied. Therefore, these variables, together with the number of layers and t, are those that should be better defined in order to obtain the best-sized and optimized prosthesis possible.

As a complement to the analyses of the effects of each response separately, there was a correlation analysis between them. Figure 10 displays the result indicating the Pearson correlation coefficients of the mass (var1) and Tsai–Wu index (var2) responses. The results indicate, as expected, that the responses are not correlated. Furthermore, it is known that these responses, when treated in optimization formulation, are conflicting objective functions, ideas to be treated in multi-objective optimization problems.

4.2 Multi-objective optimization results

As previously discussed, simulations were performed with the four optimizers, MOLA, NSGA—II, MOSFO, and MOPSO. After having performed the optimizations, the

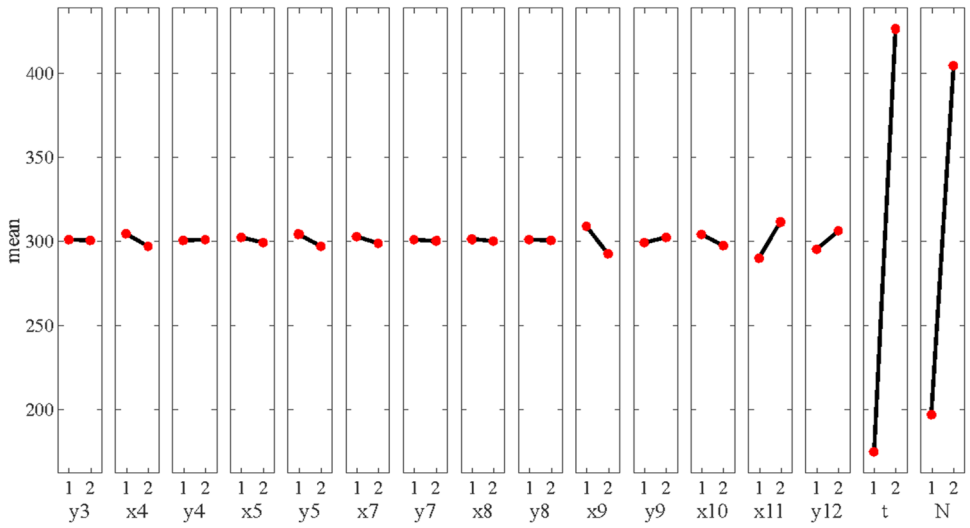

Fig. 8 Main effects of decision variables on mass response

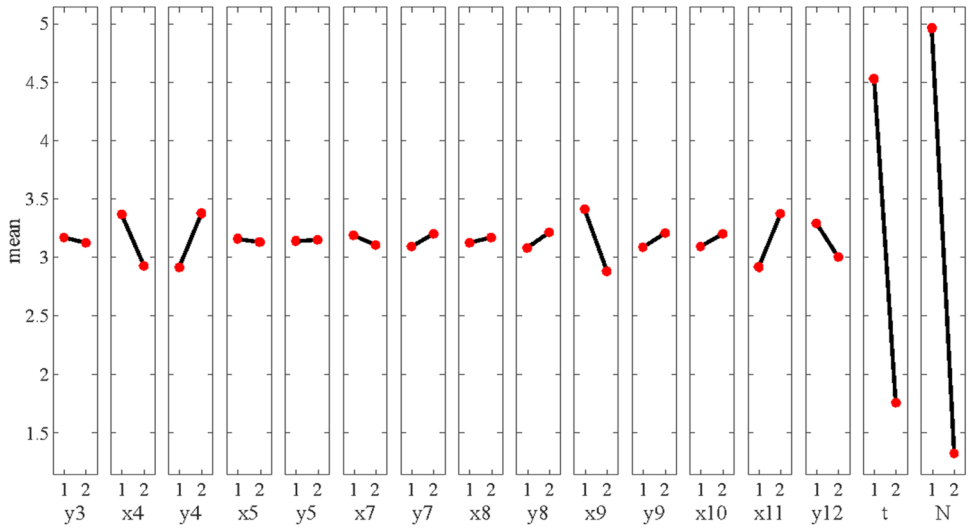

Fig. 9 Main effects of the decision variables on the Tsai–Wu response

Pareto fronts were generated for all four optimizers in the two loading conditions (case #1 and case #2), and it is possible to discuss which ones obtained the best answers for the problem studied.

4.2.1 Case #1: strength on the prosthesis tip

The first case is that of a strength applied on the tip of the prosthesis (analogous to the human finger toe region), as already mentioned in Sect. 4.1. For this boundary condition (case #1) different optimal solutions were obtained considering the four optimization algorithms. The non-dominated solutions in the Pareto Front for each optimizer are visualized in Fig. 11.

It can be noted that the optimizer with which the best answers were obtained, that is, its Pareto front dominates the others generated by the other optimizers, for this case was the MOPSO (multi-objective particle swarm algorithm). In turn, although the other optimizers present Pareto fronts with solutions that meet the loading conditions in the prosthesis, the results obtained by them are not the most optimized for the two objective functions considered in this study.

As a criterion for analysis, we obtained the images of the simulated prostheses with the geometries obtained by the optimizers. The answers sought were those corresponding to the nadir points on the Pareto front, it means, the prosthesis configurations that have individual objectives optimized only one criterion. In addition, the best non-dominated solution on each front was also sought using the TOPSIS (Technique for Order Preference by Similarity to Ideal Solution) method for decision making that equally weights the importance of the Tsai–Wu mass and failure index objectives.

Figure 12 shows the different structural designs of the prostheses considering the nadir and TOPSIS points for the

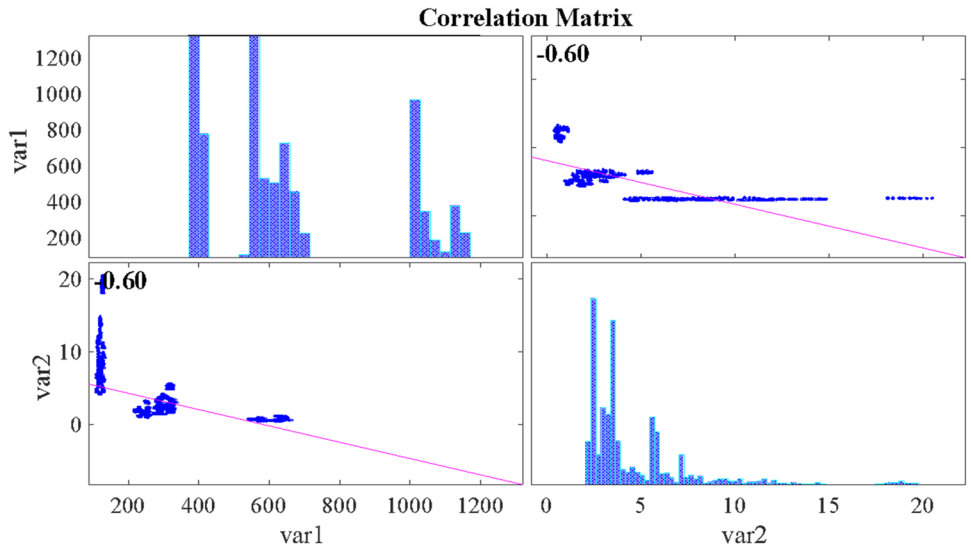

Fig. 10 Correlation between the responses mass (var1) and Tsai–Wu (var2)

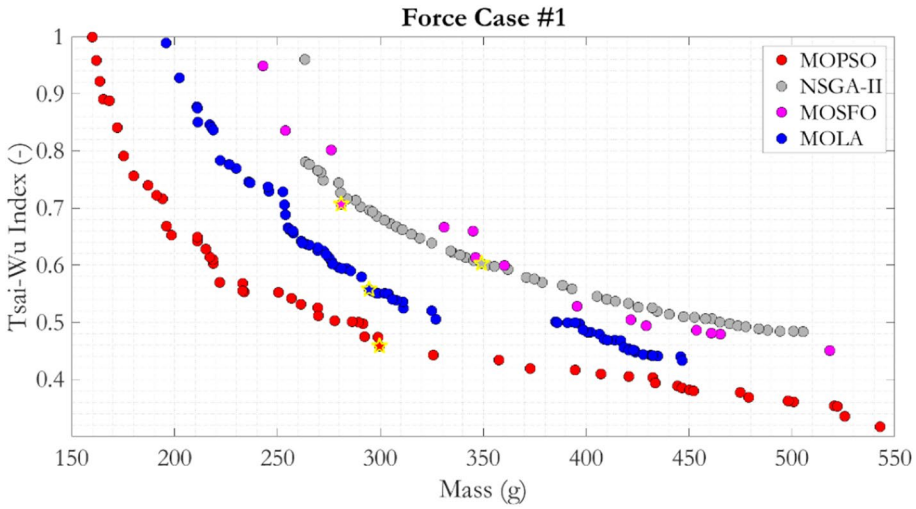

Fig. 11 Pareto front obtained in the multi-objective optimization for boundary condition 1

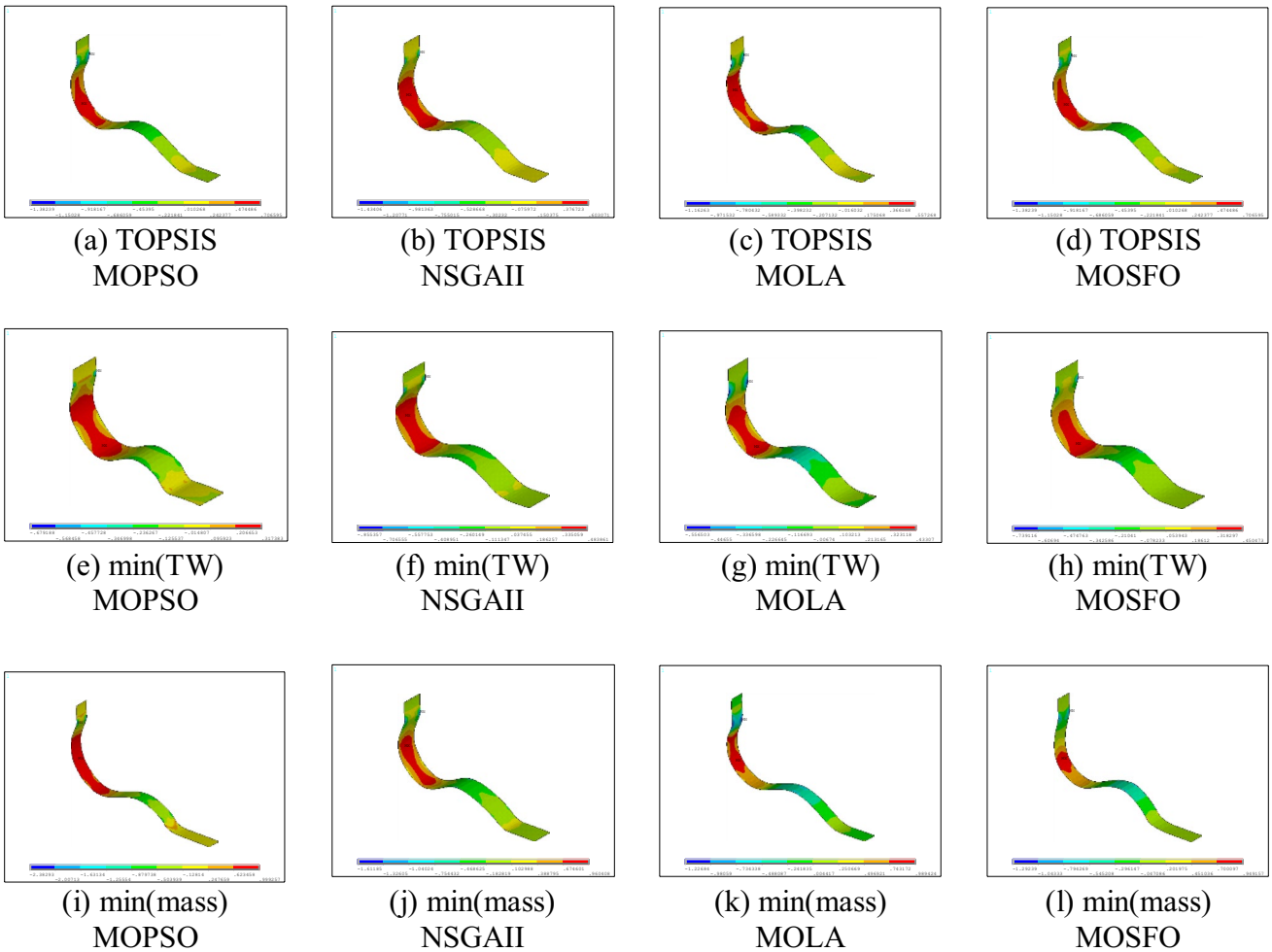

Fig. 12 Optimal forms obtained from the non-dominated Pareto front solutions for boundary condition I

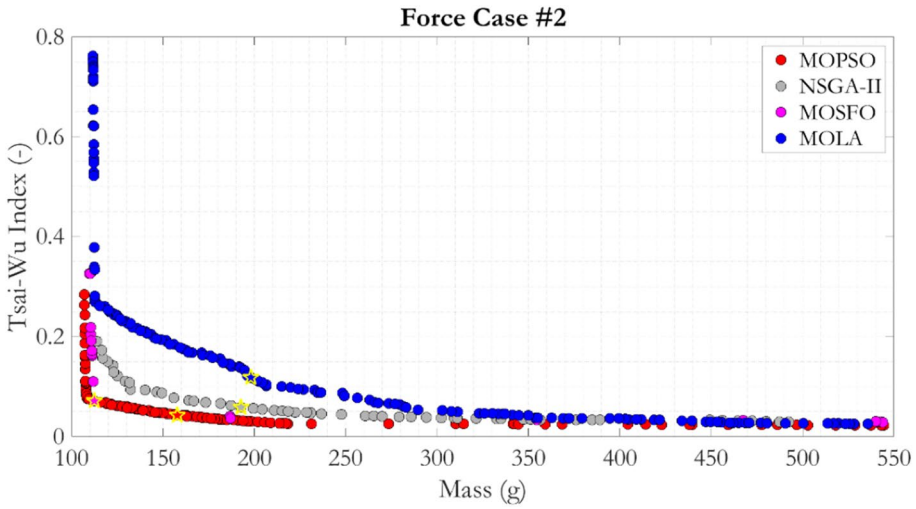

Fig. 13 Pareto front obtained in multi-objective optimization for boundary condition II

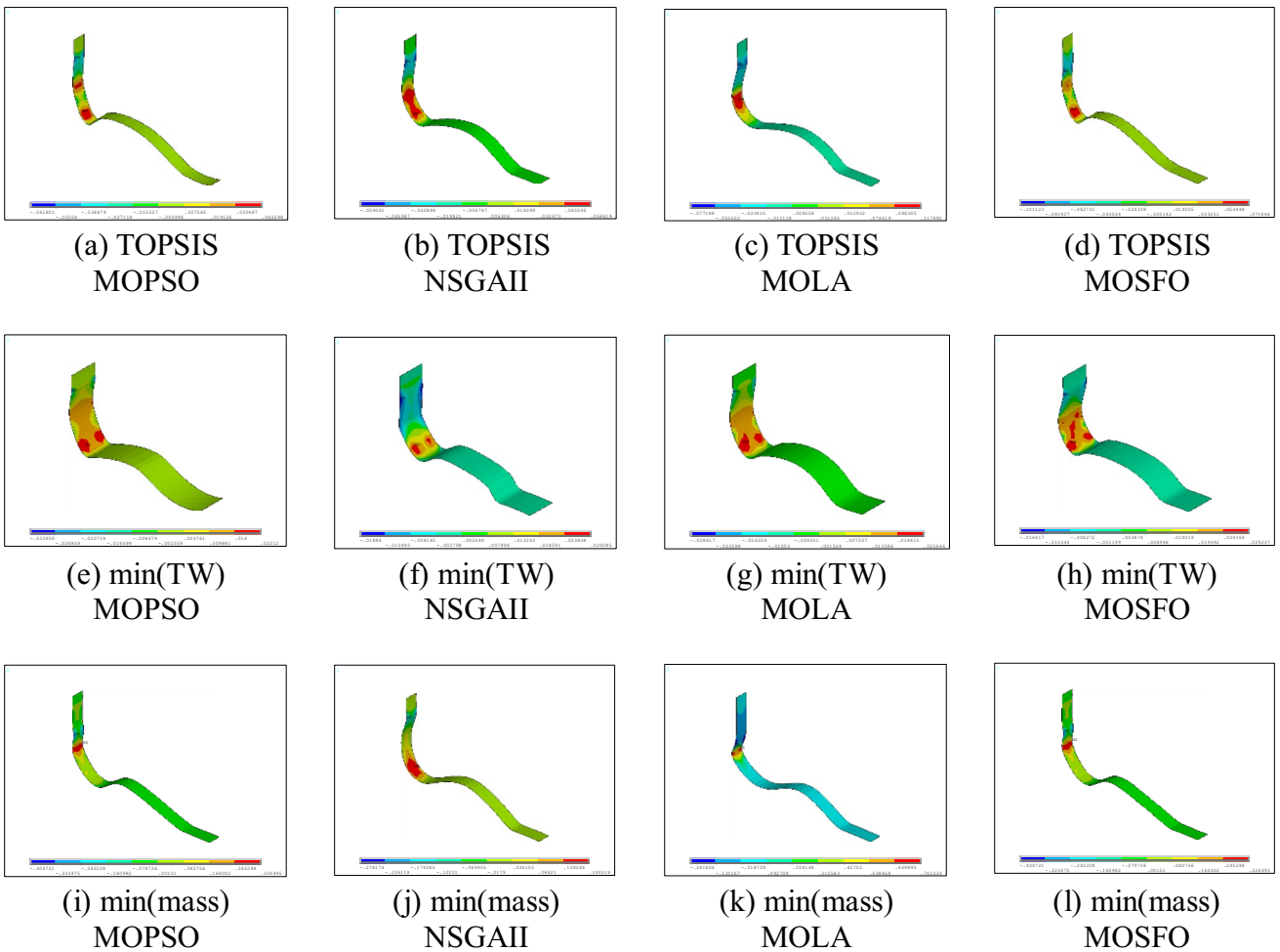

Fig. 14 Optimal forms obtained from the non-dominated Pareto front solutions for boundary condition II

Table 4 Optimization metrics obtained for case I and II considering the different algorithms

Case	Algorithms	HV	TOPSIS		Nadir	
			Mass (g)	TW (−)	Mass (g)	TW (−)
I	MOPSO	**0.7869**	299.60	**0.4578**	**159.92**	**0.3174**
	NSGA-II	0.7374	349.14	0.6031	263.21	0.4838
	MOLA	0.7375	294.58	0.5572	195.87	0.4331
	MOSFO	0.7281	**280.88**	0.7066	243.03	0.4504
II	MOPSO	**0.9867**	157.93	**0.0422**	**107.02**	**0.0221**
	NSGA-II	0.9782	192.72	0.0586	113.73	0.0292
	MOLA	0.9663	198.19	0.1179	111.62	0.0256
	MOSFO	0.9817	**112.29**	0.0716	109.74	0.0284

different metaheuristics evaluated. Note that, as expected, the prostheses that prioritize mass reduction have a less robust structure than those that prioritize TW reduction. And in turn, the TOPSIS solution becomes an equilibrium of the two objective functions which for the present study is considered the sweet spot.

4.2.2 Case #2: strength on the heel of the prosthesis

The second case considered as boundary condition the strength applied in the heel region of the prosthesis with a total load of 500 kg. The analysis was performed similarly to Case 1. Figure 13 exhibits the non-dominated solutions that were the Pareto fronts for the four different optimizers considered.

Similar to the result obtained for the first boundary condition, the simulation with the load on the tip of the prosthesis, the optimizer that best minimized the mass and TW was MOPSO. However, with the load applied to the heel it was possible to obtain "lighter" prostheses, since the geometry allows for a greater load applied to this region of the prosthesis. Figure 14 shows in detail the structural profiles of the prosthesis considering the different nadir and TOPSIS solutions for the four metaheuristics.

As commented, with this load the prosthesis suffered less, so the optimizers were able to arrive at less robust geometries, unlike what happened in the prostheses with the tip load.

Complementing the previous results, Table 4 summarizes the metrics obtained for cases 1 and 2 studies considering all the algorithms involved. It can be observed that the MOPSO algorithm was the metaheuristic that presented the best performance for this specific problem. When only the Nadir solutions are taken into account, the MOSFO algorithm showed a slight advantage over MOPSO. Evaluating the hypervolume (HV) metric obtained by the Pareto front, once again the MOPSO algorithm presents an advantage over the others. The best values are highlighted in bold.

5 Conclusions

Taking into account the findings of this study, which involved simulating two different stress conditions and testing four optimization algorithms (MOLA, NSGA-II, MOSFO, and MOPSO), it can be seen that the prosthesis that would best meet the loading conditions is the one obtained by the MOPSO optimizer for the load on the tip of the structure, once this boundary condition was the one that required more robustness in the prosthesis. Soon, just as it performed well in condition (I), it would also perform effectively with a load on the heel, condition (II). Moreover, as already mentioned, it also has a more convex Pareto front than the other optimizers, which generated a better decision making and TOPSIS solution. This metaheuristic provided the highest hypervolume index among the others studied, adding one more advantage for this prosthesis among the others.

Acknowledgements The authors would like to acknowledge the financial support from the Brazilian agency CNPq (Conselho Nacional de Desenvolvimento Científico e Tecnológico—431219/2018-4), CAPES (Coordenacão de Aperfeicoamento de Pessoal de Nível Superior), and FAPEMIG (Fundacão de Amparo à Pesquisa do Estado de Minas Gerais—APQ-00385-18).

Declarations

Conflict of interest The authors declare no conflict of interest.

Replication of results The raw/processed data required to reproduce these findings cannot be shared at this time as the data also form part of an ongoing study.

References

Carbonaro D, Gallo D, Morbiducci U, Audenino A, Chiastra C (2021) In silico biomechanical design of the metal frame of transcatheter aortic valves: multi-objective shape and cross-sectional size optimization. Struct Multidisc Optim 64(4):1825–1842

Chanda S, Gupta S, Pratihar DK (2016) Effects of interfacial conditions on shape optimization of cementless hip stem: an investigation based on a hybrid framework. Struct Multidisc Optim 53(5):1143–1155

Coello CAC (2000) Use of a self-adaptive penalty approach for engineering optimization problems. Comput Ind 41:113–127

Diniz CA, Cunha SS, Gomes GF, Ancelotti AC (2019) Optimization of the layers of composite materials from neural networks with Tsai–Wu failure criterion. J Fail Anal Prev 19:709–715

Fonseca CM, Fleming PJ (1993) Genetic algorithms for multi-objective optimization: formulation discussion and generalization. In: Proceedings of the International Conference on Genetic Algorithms, vol 93. Citeseer. pp 416–423

Francisco MB, Pereira JLJ, Oliver GA, da Silva FHS, da Cunha Jr SS, Gomes GF (2021) Multi-objective design optimization of CFRP isogrid tubes using sunflower optimization based on metamodel. Comput Struct 249:106508

Gomes GF, de Almeida FA (2020) Tuning metaheuristic algorithms using mixture design: application of sunflower optimization for structural damage identification. Adv Eng Softw 149:102877

Gomes GF, da Cunha SS, Ancelotti AC (2019) A sunflower optimization (SFO) algorithm applied to damage identification on laminated composite plates. Eng Comput 35(2):619–626

Kaveh A, Laknejadi K (2011) A novel hybrid charge system search and particle swarm optimization method for multi-objective optimization. Expert Syst Appl 38(12):15475–15488

Kaveh A, Laknejadi K (2013) A new multi-swarm multi-objective optimization method for structural design. Adv Eng Softw 58:54–69

Kazunori H, Hiroto T, Satoshi K, Goro O (2019) Parametric modeling of sports prostheses based on the flat spring design formulas. J Biomech Sci Eng 15:1900446

Light C, Chappell P (2000) Development of a lightweight and adaptable multiple-axis hand prosthesis. Med Eng Phys 22(10):679–684

Ma Y, Chen X, Zuo W (2020) Equivalent static displacements method for contact force optimization. Struct Multidisc Optim 62(1):323–336

Oudenhoven LM, Boes JM, Hak L, Faber GS, Houdijk H (2017) Regulation of step frequency in transtibial amputee endurance athletes using a running-specific prosthesis. J Biomech 51:42–48

Pereira JLJ, Francisco MB, Diniz CA, Oliver GA, Cunha SS, Gomes GF (2021a) Lichtenberg algorithm: a novel hybrid physics-based meta-heuristic for global optimization. Expert Syst Appl 170:114522

Pereira JLJ, Francisco MB, Cunha SS Jr, Gomes GF (2021b) A powerful Lichtenberg optimization algorithm: a damage identification case study. Eng Appl Artif Intell 97:104055

Pereira JLJ, Francisco MB, Ribeiro RF, Cunha SS, Gomes GF (2022a) Deep multi-objective design optimization of CFRP isogrid tubes using lichtenberg algorithm. Soft Comput 26(15):7195–7209

Pereira JLJ, Oliver GA, Francisco MB, Cunha SS, Gomes GF (2022b) Multi-objective lichtenberg algorithm: a hybrid physics-based meta-heuristic for solving engineering problems. Expert Syst Appl 187:115939

Perl DP, Daoud AI, Lieberman DE (2012) Effects of footwear and strike type on running economy. Med Sci Sports Exerc 44(7):1335–1343

Rosel Solis MJ, Dávalos Ramírez JO, Molina Salazar J, Ruiz Ochoa JA, Gómez Roa A (2021) Optimization of running blade prosthetics utilizing crow search algorithm assisted by artificial neural networks. Strojniski Vestnik/j Mech Eng 67(3):88

Ruben RB, Folgado J, Fernandes PR (2007) Three-dimensional shape optimization of hip prostheses using a multicriteria formulation. Struct Multidisc Optim 34(3):261–275

Shepherd MK, Gunz D, Clites T, Lecomte C, Rouse EJ (2022) Designing custom mechanics in running-specific prosthetic feet via shape optimization. IEEE Transact Biomed Eng 70:747

Tamiris Costa L et al (2019) Qualidade de vida de protetizados de membro inferior. SALUSVITA, Bauru, pp 881–897

Tao Z, Ahn HJ, Lian C, Lee KH, Lee CH (2017) Design and optimization of prosthetic foot by using polylactic acid 3D printing. J Mech Sci Technol 31(5):2393–2398

Tryggvason H, Starker F, Lecomte C, Jonsdottir F (2020) Use of dynamic FEA for design modification and energy analysis of a variable stiffness prosthetic foot. Appl Sci 10(2):650

Venkadesan M, Yawar A, Eng CM, Dias MA, Singh DK, Tommasini SM, Mandre S (2020) Stiffness of the human foot and evolution of the transverse arch. Nature 579(7797):97–100

Yang X-S (2014) Nature-inspired optimization algorithms. Elsevier, Amsterdam